JOURNAL OF THERMOPHYSICS AND HEAT TRANSFER
Vol. 24, No. 3, July–September 2010

# Technical Notes

## Variable Thermal Conductivity and Perforation Effects on a Heat-Conducting Plate

J. C. Cajas*
*Universidad Nacional Autónoma de México, 04510 México, D.F., México*
C. Treviño†
*Universidad Nacional Autónoma de México, 97356, Sisal, Yucatán, México*
and
J. Lizardi‡
*Universidad Autónoma de la Ciudad de México, 09790 México, D.F., México*

DOI: 10.2514/1.46888

### I. Introduction

THE heat transfer across irregular surfaces, such as perforated plates, has been extensively studied in the past to control the rate of thermal energy in heat exchanger devices. In some cases the use of perforated plates within ranges of temperature at which the material that constitutes the plate exhibits a temperature-dependent thermal conductivity is unavoidable. This makes necessary the study of the influence of variable thermal conductivity of perforated plates on heat conduction processes in order to improve the design and construction of the involved equipments.

Over the past years, important research efforts have been devoted to the study of surfaces with circular and elliptical perforations for the design of plate fin and tube heat exchangers, like those of Romero-Méndez et al. [1], Mon and Gross [2], Erek et al. [3], and Wu and Tao [4]. Experimental research has been developed in the works of Kim and Song [5] and Saboya and Saboya [6]. Also, remarkable numerical studies have been done for the problem of heat conduction over surfaces with complex geometries like the one of Blyth and Pozrikidis [7], in which the heat conduction over irregular and fractal-like surfaces is analyzed.

In the analysis of combustible flow around catalytic wires of circular section, the geometry of the system is similar to the one studied in the present work, making possible the use of the methods applied to such problems, like those found in the work of Vera and Liñán [8], and that of Lizardi et al. [9], who studied combustion problems around catalytic wires.

In the study of the effects of variable thermal conductivity in heat transfer processes, a great advance in research is achieved. Representative works are those of Hung and Appl [10], Aziz and Hug [11], Krane [12], Muzzio [13], Aziz and Benzies [14], and Aziz and Na [15], who have extensively applied regular perturbation techniques to clarify the role of variable thermal conductivity on the performance of longitudinal fins. Chiu and Chen [16] used a decomposition method to evaluate the efficiency and the optimal length of a convective fin with variable thermal conductivity. Later, Lizardi et al. [17] studied the conjugate film condensation heat transfer process in a vertical fin with temperature-dependent thermal conductivity using perturbation techniques and numerical calculations.

In this Note, the effect of a circular perforation combined with that of a variable thermal conductivity in a heat-conducting rectangular plate is studied.

### II. Problem Formulation

The physical model under study is shown in Fig. 1. A rectangular plate of length $2L^*$, width $2a^*$ with a circular perforation of radius $\varepsilon^*$ at the center is considered. Here, the superscript $*$ stands for dimensional quantities. The Cartesian coordinates $x^*$ and $y^*$ represent the longitudinal and transverse directions, respectively. The perforation, the upper and lower boundaries of the plate ($y^* = \pm a^*$) are assumed to be adiabatic, while the other two boundaries are assumed to be in contact with thermal reservoirs at different temperatures $T_0^*$ at $x^* = -L^*$ and $T_1^*$ at $x^* = +L^*$, with $T_0^* < T_1^*$ without loss of generality. The thermal conductivity of the plate, $k^*(T^*)$, is considered to exhibit a linear variation with temperature, which is common for different materials in a restricted temperature range. In this case, the nondimensional thermal conductivity $k(\theta)$ can be written as

$$k(\theta) = k^*(T^*)/k_0^* = 1 + \lambda\theta \tag{1}$$

where $k_0^*$ is the thermal conductivity of the plate at temperature $T^* = T_0^*$. $\lambda$ is defined as $\lambda = (T_1^* - T_0^*)/k_0^*(\mathrm{d}k^*/\mathrm{d}T^*)_0$, which measures the variation of thermal conductivity with temperature and can be positive or negative, depending on the material of the plate and $\theta$ is the nondimensional normalized temperature difference $\theta = (T^* - T_0^*)/(T_1^* - T_0^*)$. Thus, considering that no heat sources or sinks exists and the steady state is reached, the heat equation for this problem, in nondimensional form is given by

$$(1 + \lambda\theta)\nabla^2\theta + \lambda\nabla\theta \cdot \nabla\theta = 0 \tag{2}$$

where both coordinates are scaled with the width $a^*$. Taking advantage of the symmetry of the problem, the above equation can be solved only for the upper half of the plate, with the following boundary conditions:

$$\begin{aligned} &\theta(-L, y) = \theta(L, y) - 1 = \left.\frac{\partial\theta}{\partial y}\right|_{y=1} = 0 \qquad , \left.\frac{\partial\theta}{\partial y}\right|_{y=0} = 0 \\ &x \in (-L, -\varepsilon) \cup (\varepsilon, L), \qquad \left.\frac{\partial\theta}{\partial r}\right|_{r=\varepsilon} = 0, \qquad x \in (-\varepsilon, \varepsilon) \end{aligned} \tag{3}$$

Here, $L$ is the aspect ratio of the plate $L = L^*/a^*$, $\varepsilon$ is the nondimensional radius of perforation $\varepsilon = \varepsilon^*/a^*$, and $r$ is the usual polar nondimensional radial coordinate $r = \sqrt{x^2 + y^2}$.

To measure the influence of the perforation and the variable thermal conductivity, the longitudinal overall heat flux in the plate,

$$Q^* = 2\int_0^{a^*} k^*\partial T^*/\partial x^*|\,\mathrm{d}y^*$$

is calculated using the average Nusselt number, defined as

Received 28 August 2009; revision received 24 February 2010; accepted for publication 12 March 2010. 

*Facultad de Ciencias; jc_cajas@ciencias.unam.mx.
†Facultad de Ciencias y Unidad Multidisciplinaria de Docencia e Investigación.
‡Colegio de Ciencia y Tecnología.

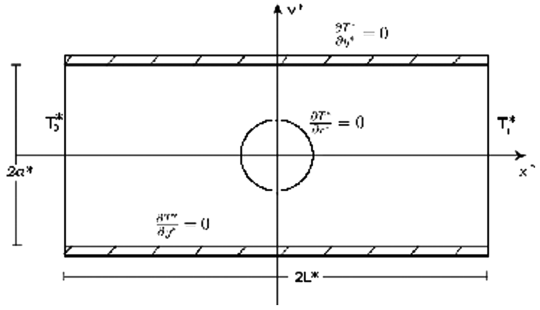


**Fig. 1 Schematic diagram of the problem.**

$$\bar{N}u = \frac{Q^*}{2k_0^*(T_1^* - T_0^*)} = \int_0^1 k(\theta)\frac{\partial\theta}{\partial x}\,\mathrm{d}y = \int_0^1 (1+\lambda\theta)\frac{\partial\theta}{\partial x}\,\mathrm{d}y \quad (4)$$

which is independent of the longitudinal coordinate $x$.

## III. Numerical Method

A coordinate fitted grid generator was developed in order to obtain a computational domain that permitted to map the complex physical geometry of the problem in a simpler rectangular one. Figure 2 shows a schematic representation of the mapping.

In the grid generation technique used in this work, the coordinates $(x, y)$ of the physical domain are obtained as the solution of a system of partial differential equations with Dirichlet boundary conditions and are functions of the rectangular transformed coordinates $(\xi, \eta)$ [18]. In this Note, Poisson's equations were used in order to generate the grid, and the boundary conditions imposed were those that corresponded to the shape and size of the perforated plate.

The governing equation is transformed to the rectangular domain, obtaining a nonlinear partial differential equation for the dimensionless temperature $\theta$ as functions of the rectangular coordinates $(\xi, \eta)$:

$$\alpha\frac{\partial^2\theta}{\partial\xi^2} + \gamma\frac{\partial^2\theta}{\partial\eta^2} - 2\beta\frac{\partial^2\theta}{\partial\xi\partial\eta} + \tau\frac{\partial\theta}{\partial\xi} + \sigma\frac{\partial\theta}{\partial\eta} + \frac{\lambda}{1+\lambda\theta}\left(\alpha\left(\frac{\partial\theta}{\partial\xi}\right)^2 - 2\beta\frac{\partial\theta}{\partial\xi}\frac{\partial\theta}{\partial\eta} + \gamma\left(\frac{\partial\theta}{\partial\eta}\right)^2\right) = 0 \quad (5)$$

where $\alpha$, $\beta$, $\gamma$, $\sigma$, and $\tau$ are transformation coefficients that are calculated from the generated grid. The explicit form of these coefficients and the details of the grid generation technique can be found elsewhere [9].

Uniform increments in both directions $\Delta\xi = 1/80$ and $\Delta\eta = 1/64$ were employed to discretize Eq. (5). Smaller space increments did not provide significant difference in heat transfer calculation (less than 1%). Using a fictitious time with increments of the order of $\Delta\xi\Delta\eta$, the transient form of Eq. (5) is solved in an semi-implicit form, by discretizing using centered finite differences. This procedure converts the transformed governing equation in a system of algebraic equations for both directions $\xi$ and $\eta$. Each system of algebraic equations is arranged in the form of a tridiagonal matrix and solved by the use of an iterative procedure and a well known tridiagonal matrix solver. The nonlinear terms are calculated from a previous iteration. The iterative procedure stops when the convergence criteria (maximum difference between results of different iterations less than $10^{-8}$) is achieved. The boundary conditions are imposed by fixing the values of the first and last rows of each tridiagonal matrix.

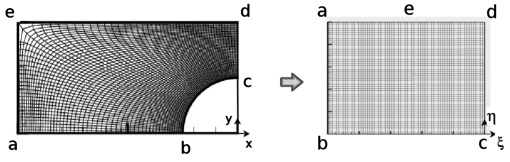


**Fig. 2 Schematic representation of coordinate transformation.**

## IV. Asymptotic Solution

Assuming values of the nondimensional radius of perforation $\varepsilon$ and the parameter $\lambda$ to be very small compared with unity, it is possible to use the focus of the complex potential, which is usually employed in the description of flow around spheres or cylinders [8]. In the case of constant thermal conductivity $\lambda = 0$, Eq. (2) becomes Laplace's equation, and its solution can be obtained using the complex potential of a linear array of point-sources dipoles located at the points $(0, 2n)$, with $n = \pm1, \pm2, \ldots$, and a constant heat flux. In this manner, the solution of Laplace equation with the boundary conditions (3) up to order $\varepsilon^4$ is

$$\theta_0(x,y) = \frac{1}{2} + \left(1 - \frac{\pi\varepsilon^2}{2L} + \frac{\pi^2\varepsilon^4}{4L^2} - \frac{\pi^3\varepsilon^4}{24L}\right)\frac{x}{2L} + \left(\frac{\pi\varepsilon^2}{4L} + \frac{\pi^3\varepsilon^4}{48L} - \frac{\pi^2\varepsilon^4}{8L^2}\right)\frac{\sinh(\pi x)}{\cosh(\pi x) - \cos(\pi y)} + \mathcal{O}(\varepsilon^6) \quad (6)$$

In the case of linear variation of thermal conductivity with temperature, a solution of the form $\theta = \theta_0 + \lambda\theta_1 + \lambda^2\theta_2$ is proposed for Eq. (2), substituting and keeping only terms of first order in $\lambda$ an equation for $\theta_1$ is obtained,

$$\nabla^2\theta_1 = \frac{1}{4L^2} + \frac{\pi\varepsilon^2}{4L^2}\left(\frac{1}{L} - \pi\frac{1 - \cosh(\pi x)\cos(\pi y))}{(\cosh(\pi x) - \cos(\pi y))^2}\right) + \mathcal{O}(\varepsilon^4) \quad (7)$$

to be solved with the following homogeneous boundary conditions:

$$\theta_1(L,y) = \theta_1(-L,y) = 0, \qquad \left.\frac{\partial\theta_1}{\partial y}\right|_{y=0} = \left.\frac{\partial\theta_1}{\partial y}\right|_{y=1} = 0 \quad (8)$$

The solution of Eq. (7) is given by

$$\theta_1(x,y) = \left(\frac{1}{8} - \frac{x^2}{8L^2}\right) + \frac{\pi\varepsilon^2 x}{8L^2}\left(\frac{x}{L} - \frac{\sinh(\pi x)}{\cosh(\pi x) - \cos(\pi y)}\right) + \mathcal{O}(\varepsilon^4) \quad (9)$$

Finally, the solution for Eq. (2) is

$$\theta(x,y) = \frac{1}{2} + \left(1 - \frac{\pi\varepsilon^2}{2L} + \frac{\pi^2\varepsilon^4}{4L^2} - \frac{\pi^3\varepsilon^4}{24L}\right)\frac{x}{2L} + \left(\frac{\pi\varepsilon^2}{4L} + \frac{\pi^3\varepsilon^4}{48L} - \frac{\pi^2\varepsilon^4}{8L^2}\right)\frac{\sinh(\pi x)}{\cosh(\pi x) - \cos(\pi y)} + \frac{\lambda}{8}\left(1 - \frac{x^2}{L^2}\right) + \frac{\lambda\pi\varepsilon^2 x}{8L^2}\left(\frac{x}{L} - \frac{\sinh(\pi x)}{\cosh(\pi x) - \cos(\pi y)}\right) + \frac{\lambda^2}{16}\left(1 + \frac{x}{L}\right)^2\left(1 - \frac{x}{L}\right) + \mathcal{O}(\varepsilon^6, \lambda\varepsilon^4, \lambda^3) \quad (10)$$

where only the leading-order term is retained for $\theta_2$. From Eqs. (4) and (10) the average Nusselt number is calculated up to terms of order $\mathcal{O}(\varepsilon^4, \lambda\varepsilon^2)$ and is given by

$$\bar{N}u = \frac{1}{2L}\left[1 - \frac{\pi\varepsilon^2}{2L}\right]\left(1 + \frac{\lambda}{2}\right) + \frac{1}{2L}\left[\frac{\pi^2\varepsilon^4}{4L^2}\left(1 - \frac{\pi L}{6}\right)\right] + \mathcal{O}(\varepsilon^6, \lambda\varepsilon^4) \quad (11)$$

## V. Numerical Results

The numerical method was applied to plates of three different aspect ratios $L = 3/2$, 2, and 5/2, with 16 different radii of perforation between $\varepsilon = 0.01$ and 0.75. The values of the nondimensional thermal conductivity parameter $\lambda$ studied were 0.55, 0.10, 0.00, −0.05, and −0.10. Figures 3 and 4 show the numerical result for the average Nusselt number $\bar{N}u$ for the three aspect ratios as a function of the radius of perforation for $\lambda = 0.55$, and −0.10, corresponding to a stainless steel and a platinum plate between thermal reservoirs at 100 and 200°C. The average Nusselt number

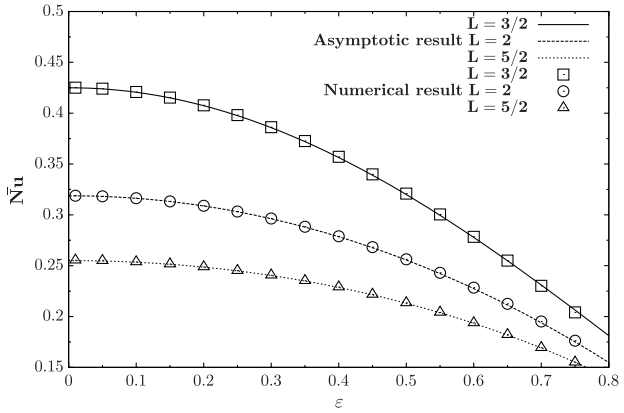


**Fig. 3 Average Nusselt number for $\lambda = 0.55$.**

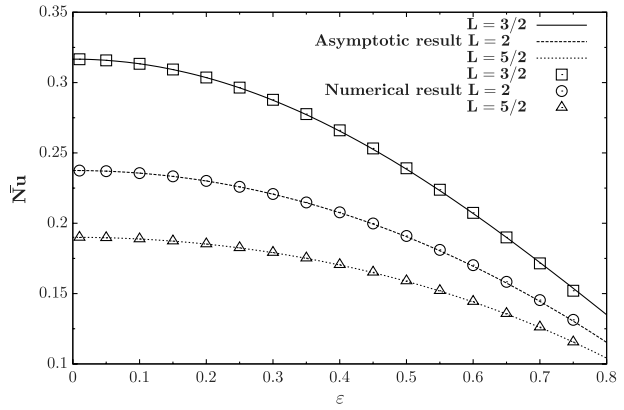


**Fig. 4 Average Nusselt number for $\lambda = -0.10$.**

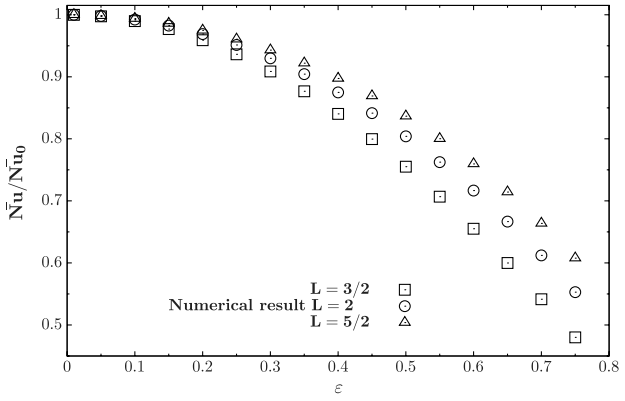


**Fig. 5 Normalized average Nusselt number for $\lambda = 0$.**

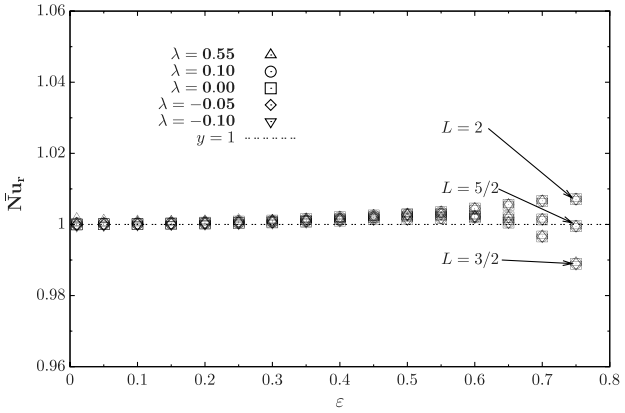


**Fig. 6 Reduced average Nusselt number.**

decreases with the size of the perforation as predicted by the asymptotic solution given by Eq. (11). In fact, the asymptotic solution obtained for small values of $\varepsilon$ gives excellent results for values of $\varepsilon$ up to 0.75. It is to be noted that for a value of the aspect ratio of $L = 6/\pi$ the correction of order $\epsilon^4$ vanishes identically.

To compare the effect of the radius of perforation on the heat conduction in plates with the same thermal conductivity parameter $\lambda$ but different aspect ratios $L$, the average Nusselt number can be normalized with the value of the corresponding average Nusselt number for a rectangular plate without perforation, $\bar{Nu}_0$. A typical result for this normalized average Nusselt number is shown in Fig. 5. The plot indicates that the negative effect on the heat transfer is independent of the aspect ratio of the plate for small values of the radius of perforation up to $\varepsilon = 0.1$, meanwhile for larger values of $\varepsilon$ the negative effect is greater for plates with smaller aspect ratios and is smaller for plates with larger aspect ratios.

As dictated by the asymptotic solution given by Eq. (11), a reduced averaged Nusselt number can be defined as

$$\bar{Nu}_r = \frac{2L\bar{Nu}}{[1 - \frac{\pi\varepsilon^2}{2L} + \frac{\pi^2\varepsilon^4}{4L^2}(1 - \frac{\pi L}{6})](1 + \frac{\lambda}{2})} \tag{12}$$

where an appropriate factorization has been used. Figure 6 shows the plot for $\bar{Nu}_r$ as a function of $\varepsilon$ for all values of parameter $\lambda$ and for all aspect ratios of the plates considered in this work. The plot shows that the effect of a thermal conductivity that varies with temperature in the form of Eq. (1) affects the heat transfer on the plate by including an overall factor $(1 + \lambda/2)$, making $\bar{Nu}_r$ almost independent of the value of $\lambda$. This result was expected, given that thermal conductivity is a property of the material of the plate and is independent of its shape. The reduced Nusselt number is independent of $\varepsilon$ for all the studied values (the maximum difference is of order 1% for $\varepsilon = 0.75$), which indicates that the asymptotic solution is valid in all these cases.

The effect of the perforation over the temperature distribution in the upper limit of the plate is shown in the Fig. 7 for the extreme case of $\lambda = 0.55$, other cases follow the same trends. The effect of three different values of the nondimensional radius ($\varepsilon = 0.01$, $\varepsilon = 0.40$ and $\varepsilon = 0.75$) are compared. For small radius of perforation, the temperature distribution is close to the corresponding to a rectangular plate without perforation. When the radius of perforation becomes greater, the temperature distribution is deformed and a region of greater thermal stress is created.

Comparing the final results for average Nusselt number equation (11) for the cases $\lambda = 0$ and $\varepsilon = 0$,

$$\bar{Nu}(\varepsilon, L, \lambda = 0) = \frac{1}{2L}\left[1 - \frac{\pi\varepsilon^2}{2L} + \frac{\pi^2\varepsilon^4}{4L^2}\left(1 - \frac{\pi L}{6}\right)\right] + \mathcal{O}(\varepsilon^6)$$

$$\bar{Nu}(\varepsilon = 0, L, \lambda) = \frac{1}{2L}\left(1 + \frac{\lambda}{2}\right)$$

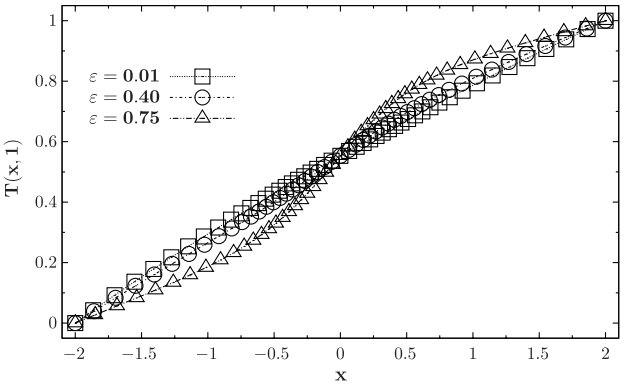


**Fig. 7 Temperature in the upper limit of the plate for $\lambda = 0.55$.**

it is possible to conclude that a perforated plate with radius of perforation $\varepsilon$ can be considered as a nonperforated plate with a variable thermal conductivity with thermal conductivity parameter $\lambda = -\pi\varepsilon^2/L + \pi^2\varepsilon^4(1 - \pi L/6)/(2L^2)$, giving a nondimensional thermal conductivity of the form

$$k(\theta) = 1 + \left(\frac{-\pi\varepsilon^2}{L} + \frac{\pi^2\varepsilon^4}{2L^2}\left(1 - \frac{\pi L}{6}\right)\right)\theta \tag{13}$$

which reminds Einstein's law for viscosity. This suggests that a general law for the effect of circular perforations on the heat transfer process across a rectangular plate, similar to that of the viscosity of a fluid, can be obtained as a generalization of the present work.

## VI. Conclusions

In this work both numerical and asymptotic analyses have been done in order to obtain the influence of circular perforations and variable thermal conductivity on the overall heat transfer rate of a rectangular plate. The asymptotic analysis gives excellent results for all the values of the ratio of the perforation radius to the half-width of the plate and for all values of $\lambda$ considered. Thus an excellent analytic description of the overall nondimensional heat flux (Nusselt number) is provided by Eq. (11).

## References

[1] Romero-Méndez, R., Sen, M., Yang, K. T., and McClain, R., "Effect of Fin Spacing on Convection in a Plate Fin and Tube Heat Exchanger," *International Journal of Heat and Mass Transfer*, Vol. 43, No. 1, 2000, pp. 39–51. doi:10.1016/S0017-9310(99)00120-9

[2] Mon, M. S., and Gross, U., "Numerical Study of Fin-Spacing Effects in Annular-Finned Tube Heat Exchangers," *International Journal of Heat and Mass Transfer*, Vol. 47, Nos. 8–9, 2004, pp. 1953–1964. doi:10.1016/j.ijheatmasstransfer.2003.09.034

[3] Erek, A., Ozerdem, B., Bilir, L., and Ilken, Z., "Effect of Geometrical Parameters on Heat Transfer and Pressure Drop Characteristics of Plate Fin and Tube Heat Exchangers," *Applied Thermal Engineering*, Vol. 25, No. 14–15, 2005, pp. 2421–2431. doi:10.1016/j.applthermaleng.2004.12.019

[4] Wu, J., and Tao, W., "Investigation on Laminar Convection Heat Transfer in Fin-and-Tube Heat Exchanger in Aligned Arrangement with Longitudinal Vortex Generator from the Viewpoint of Field Synergy Principle," *Applied Thermal Engineering*, Vol. 27, Nos. 14–15, 2007, pp. 2609–2617. doi:10.1016/j.applthermaleng.2007.01.025

[5] Kim, J. Y., and Song, T. H., "Microscopic Phenomena and Macroscopic Evaluation of Heat Transfer from Plate Fins/Circular Tube Assembly Using Naphthalene Sublimation Technique," *International Journal of Heat and Mass Transfer*, Vol. 45, No. 16, 2002, pp. 3397–3404. doi:10.1016/S0017-9310(02)00047-9

[6] Saboya, S. M., and Saboya, F. E. M., "Experiments on Elliptic Sections in One and Two Row Arrangements of Plate Fin and Tube Heat Exchangers," *Experimental Thermal and Fluid Science*, Vol. 24, Nos. 1–2, 2001, pp. 67–75. doi:10.1016/S0894-1777(00)00059-5

[7] Blyth, M. G., and Pozrikidis, C., "Heat Conduction Across Irregular and Fractal-Like Surfaces," *International Journal of Heat and Mass Transfer*, Vol. 46, No. 8, 2003, pp. 1329–1339. doi:10.1016/S0017-9310(02)00419-2

[8] Vera, M., and Liñán, A., "Low Peclet Number Flow of a Reacting Mixture Past an Array of Catalytic Wires," *Combustion Theory and Modelling*, Vol. 8, No. 1, 2004, pp. 97–121. doi:10.1088/1364-7830/8/1/006

[9] Lizardi, J., Treviño, C., and Liñán, A., "Ignition and Combustion of Diluted Hydrogen Mixtures in a Flow Past an Array of Catalytic Wires," *Combustion Theory and Modelling*, Vol. 11, No. 3, 2007, pp. 483–499. doi:10.1080/13647830601045158

[10] Hung, H. M., and Appl, F. C., "Heat Transfer of Thin Fins with Temperature Dependent Thermal Properties and Internal Heat Generation," *Journal of Heat Transfer*, Vol. 89, 1967, pp. 155–161.

[11] Aziz, A., and Hug, S. M. E., "Perturbation Solution for Convecting Fin with Variable Thermal Conductivity," *Journal of Heat Transfer*, Vol. 97, No. 2, 1975, pp. 300–301.

[12] Krane, R. J., "Discussion on a Previously Published Paper by Aziz A and Enamul Hug SM," *Journal of Heat Transfer*, Vol. 98, 1976, pp. 685–686.

[13] Muzzio, A., "Approximate Solution for Convective Fins with Variable Thermal Conductivity," *Journal of Heat Transfer*, Vol. 98, 1976, pp. 680–682.

[14] Aziz, A., and Benzies, Y., "Application of Perturbation Techniques to Heat-Transfer Problems with Variable Thermal Properties," *International Journal of Heat and Mass Transfer*, Vol. 19, No. 3, 1976, pp. 271–276. doi:10.1016/0017-9310(76)90030-2

[15] Aziz, A., and Na, T. A., "Periodic Heat Transfer in Fins with Variable Thermal Parameters," *International Journal of Heat and Mass Transfer*, Vol. 24,No. 8, 1981, pp. 1397–1404. doi:10.1016/0017-9310(81)90189-7

[16] Chiu, C.-H., and Chen, C.-K., "A Decomposition Method for Solving the Convective Longitudinal Fins with Variable Thermal Conductivity," *International Journal of Heat and Mass Transfer*, Vol. 45, No. 10, 2002, pp. 2067–2075. doi:10.1016/S0017-9310(01)00286-1

[17] Lizardi, J., Treviño, C., and Méndez, F., "The Influence of the Variable Thermal Conductivity of a Vertical Fin on a Laminar-Film Condensation Process," *Heat and Mass Transfer*, Vol. 40, No. 5, 2004, pp. 383–391. doi:10.1007/s00231-003-0440-1

[18] Thompson, J. F., Warsi, Z. U. A., and Mastin, C. W., "Boundary-Fitted Coordinate Systems for Numerical Solution of Partial Differential Equations—A Review," *Journal of Computational Physics*, Vol. 47, No. 1, 1982, pp. 1–108. doi:10.1016/0021-9991(82)90066-3